Proc. Natl. Acad. Sci. USA
Vol. 92, pp. 7386–7390, August 1995
Medical Sciences

Atrial-like phenotype is associated with embryonic ventricular failure in retinoid X receptor α −/− mice

(transgenic mice/retinoic acid receptor/*in situ* hybridization)

EMILY DYSON*†‡§, HENRY M. SUCOV¶‖, STEVEN W. KUBALAK*†‡§, GEERT W. SCHMID-SCHÖNBEIN**, FRANK A. DELANO**, RONALD M. EVANS¶††, JOHN ROSS, JR.†, AND KENNETH R. CHIEN*†‡‡

*Center for Molecular Genetics, Division of Cardiology, †Department of Medicine, ‡American Heart Association–Bugher Foundation Center for Molecular Biology, and **Department of Bioengineering, Institute for Biomedical Engineering, University of California at San Diego, La Jolla, CA 92093; and ¶Gene Expression Laboratory, ††Howard Hughes Medical Institute, The Salk Institute for Biological Studies, La Jolla, CA 92138

Communicated by Helen M. Ranney, Alliance Pharmaceutical Corp., San Diego, CA, April 6, 1995

ABSTRACT **We have recently characterized a cardiac model of ventricular chamber defects in retinoid X receptor α (RXRα) homozygous mutant (−/−) gene-targeted mice. These mice display generalized edema, ventricular chamber hypoplasia, and muscular septal defects, and they die at embryonic day 15. To substantiate our hypothesis that the embryos are dying of cardiac pump failure, we have used digital bright-field and fluorescent video microscopy and *in vivo* microinjection of fluorescein-labeled albumin to analyze cardiac function. The affected embryos showed depressed ventricular function (average left ventricular area ejection fraction, 14%), ventricular septal defects, and various degrees of atrioventricular block not seen in the RXRα wild-type (+/+) and heterozygous (+/−) littermates (average left ventricular area ejection fraction, 50%). The molecular mechanisms involved in these ventricular defects were studied by evaluating expression of cardiac-specific genes known to be developmentally regulated. By *in situ* hybridization, aberrant, persistent expression of the atrial isoform of myosin light chain 2 was identified in the ventricles. We hypothesize that retinoic acid provides a critical signal mediated through the RXRα pathway that is required to allow progression of development of the ventricular region of the heart from its early atrial-like form to the thick-walled adult ventricle. The conduction system disturbances found in the RXRα −/− embryos may reflect a requirement of the developing conduction system for the RXRα signaling pathway, or it may be secondary to the failure of septal development.**

In the United States, one in 200 live births is affected by cardiovascular developmental anomalies, with ventricular chamber defects (hypoplasia, dysplasia, septal defects) accounting for the largest group (25–30%). Although the embryology of ventricular chamber development has been described in some detail, the molecular mechanisms that govern normal cardiac chamber growth and morphogenesis remain largely unknown. In this regard, a role for retinoids in cardiac morphogenesis has been suspected largely on the basis of previous studies of the effects of vitamin A deficiency on rat embryonic development. Vitamin A deficiency results in the onset of a specific subset of cardiovascular defects, including ventricular chamber hypoplasia, ventricular septal defects, and aortic arch anomalies (1). High concentrations of retinoic acid (RA) have been found to act as a teratogen when administered to the developing embryo (2, 3), and a well-defined retinoid embryopathy has been described in humans, which includes cardiovascular anomalies (4). Taken together, these observations support the notion that retinoids are an important morphogen that may be required as a signal for normal cardiovascular development and that, if present in an unregulated fashion, will lead to abnormal development. The genes that encode components of the retinoid signaling-dependent pathways, such as the retinoid receptors, may serve as potential candidate genes for mediating cardiovascular developmental defects seen in retinoid embryopathy and in certain forms of congenital heart disease in humans. Within this framework, downstream genes under the control of retinoid receptor pathways might be linked to specific forms of congenital heart disease in humans.

Several recent reports using gene targeting approaches have identified genes that lead to various forms of cardiovascular developmental defects in the mouse (5–10). Studies using gene targeting approaches of specific retinoid receptors in mice have now provided direct evidence that retinoids are required for normal cardiogenesis. Retinoid X receptor α (RXRα) −/− mice display midgestational lethality and prominent cardiac defects, including hypoplasia of the ventricular compact zone, muscular ventricular septal defects, and death at embryonic day 15 (E15) (10). Recently, this result has been confirmed by others and extended to suggest that RXR–RAR (RA receptor) heterodimers may mediate expansion of the compact zone and the consequent proliferation of muscle cells within the ventricular chamber at this particular stage of cardiogenesis (9, 11). Given the critical role of the growing myocardium in the maintenance of blood flow for the exponentially growing embryo, the basis of midgestational lethality has been ascribed to the concomitant decrease in ventricular function in the RXRα −/− embryos. However, direct evidence for embryonic cardiac dysfunction in any gene-targeted mouse model system has been lacking. The two major determinants of cardiac output are the stroke volume (which reflects cardiac contractile function) and the heart rate. Accordingly, any net decrease in blood flow to the growing embryo could result from a primary defect in cardiac contractile function or an effect on heart rate due to concomitant conduction system abnormalities, or a combination of these effects. At the cellular level, the decrease in cardiac contractile function could simply reflect a quantitative decrease in ventricular muscle cells due to chamber hypoplasia; alternatively, it might also result from a qualitative defect in the ventricular muscle cells. The ultimate mechanistic dissection of the molecular determinants of the RXRα −/− cardiac defect will first require a direct

The publication costs of this article were defrayed in part by page charge payment. This article must therefore be hereby marked "*advertisement*" in accordance with 18 U.S.C. §1734 solely to indicate this fact.

Abbreviations: RA, retinoic acid; RXRα, retinoid X receptor α; E, embryonic day; MLC-2, myosin light chain 2; AV, atrioventricular.

§E.D. and S.W.K. contributed equally to this work.
‖Present address: Department of Cell and Neurobiology, Institute for Genetic Medicine, University of Southern California School of Medicine, Los Angeles, CA 90033.
‡‡To whom reprint requests should be addressed at: Department of Medicine and Center for Molecular Genetics, Basic Science Building, 0613-C, University of California, San Diego School of Medicine, La Jolla, CA 92093.

analysis of the physiological phenotype and identification of molecular markers of the cardiac muscle phenotype. Thus far, characterization of cardiac phenotypes in the embryonic mouse heart have been largely confined to histological analyses, and currently no methodology is available for accessing global ventricular function and stroke volume in the mouse embryo in the *in vivo* context. Accordingly, the current study describes the application of an experimental approach to monitor cardiac physiology in the living embryo with placental circulation intact. Using this approach, these studies indicate that persistent expression of an atrial marker, atrial-specific myosin light chain 2 (MLC-2a), in the ventricle of RXRα −/− embryos correlates with the relatively thin-walled phenotype, poor trabeculation, and the onset of ventricular chamber dysfunction.

MATERIALS AND METHODS

Breeding and Identification of RXRα Gene-Targeted Mice. RXRα −/− mutant mice were maintained in colonies and bred as described (10). The genotype of individual animals was determined by PCR analysis of DNA extracted from the tail or hindlimb.

Surgical Preparation. Timed pregnant females heterozygous for the mutant RXRα gene were anesthetized with a mixture of ketamine (100 mg/kg) and xylazine (5 mg/kg) given intraperitoneally. A midline cervical incision was made to visualize the trachea and facilitate intubation, and ventilation was carried out with a rodent ventilator using room air with a respiratory vol of 0.2 ml and rate of 105–110 per min. The animal was positioned on a water-heated platform in the left lateral position on a vibration-free stage and a midline abdominal incision was made to expose the uterus. A smaller incision was then made in one horn of the uterus and a single embryo was delivered within its yolk sac and placed on a glass stage. As a reference, the heart rate was monitored briefly with a closed chest. Then, the yolk sac was opened, the upper limb buds were positioned away from the chest using moist cotton, and a portion of the cartilaginous chest wall was trimmed away. The fetus was placed in the left anterior oblique position and bright-field images of the heart were obtained by transillumination from below with a 250-W tungsten/halogen lamp equipped with infrared filters. The fetal heart and chest were continuously superfused with a Krebs–Henseleit sodium bicarbonate-buffered solution saturated with 5% CO_2/15% O_2/80% N_2 at 37°C and pH 7.4 (see Fig. 1). All embryos (n = 6–10) from each pregnant mouse were studied.

Intravital Microscopy. All four chambers of the fetal heart were visualized through an intravital microscope (Leitz) with a ×2 objective lens (numerical aperture, 0.1; Nikon, Tokyo) and a ×10 eyepiece. Images were recorded with a color CCD camera (model DEI-470; Optronics Engineering, Goleta, CA) at a shutter speed of 1/60–1/250 sec for bright-field and 1/15–1/30 sec for fluorescent images and were stored initially on a video cassette recorder at 30 images per sec (SVHS model BR 5601 Mu; JVC).

After bright-field imaging, color fluorescent images of the cardiac blood pool were obtained. A glass micropipette (tip diameter, ≈5 μm) was filled with a solution of bovine serum albumin conjugated with fluorescein isothiocyanate, and, with a micromanipulator, its tip was introduced into the left atrial chamber at the base of the atrial appendage; in some experiments, the tip was placed into the left ventricular chamber. Approximately 10–30 μl of solution was then rapidly injected while fluorescent images were recorded with a 200-W mercury lamp. The intravital microscope is equipped with a fluorescent attachment (Ploempak, Leitz) with an I-3 filter set (excitation wavelength Br, 450–490 nm; suppression filter LP, 520 nm) to illuminate the beating heart. Images were recorded on videotape as described above.

Selected fluorescent images were transferred on-line or on replay to an image digitizer (512 × 512 matrix; 8 bit deep; IMAGE 1.52 with Macintosh II_{ci} laboratory computer) and digitized images were stored on floppy or hard disc for subsequent analysis. Area ejection fractions at the left ventricle were calculated from single plane digitized images as (end diastolic ventricular area − end systolic ventricular area)/(end diastolic ventricular area).

Histological Analyses and *in Situ* Hybridization. After video microscopy of the embryo was completed, the placenta was dissected from the uterus, the embryo was removed, and the tail was clipped off for genotyping. The embryo was then fixed in 4% paraformaldehyde in phosphate-buffered saline, dehydrated, and embedded in paraffin. Serial sections (5–10 μm) were made, stained with hematoxylin and eosin, and examined by light microscopy.

For *in situ* hybridization analysis, embryos were placed in 4% paraformaldehyde in phosphate-buffered saline for fixation and further processed as described (12). RNA probes were generated and labeled with UTP[^{35}S] as described (12–14). Hybridizations, exposure, and photography were then performed (12).

Statistical Analysis. Ejection fraction data are presented as means ± SEM and were analyzed by analysis of variance followed by Student–Newman–Keuls test for detecting differences, with $P < 0.01$ considered significant.

RESULTS AND DISCUSSION

***In Vivo* Assessment of Embryonic Ventricular Function in Living Murine Embryos.** For *in vivo* assessment of murine embryonic ventricular function, digital color video microscopy was used to assess heart rate, the presence of atrioventricular (AV) conduction block, and morphology of the heart under light-field analysis. (For a depiction of the experimental setup, see Fig. 1). Pregnant females were anesthetized and intubated, an abdominal incision was made to expose the uterus, and each individual embryo was examined beginning with one horn of the uterus. After bright-field color imaging, fluorescent images of the cardiac blood pool were obtained. A contrast agent consisting of bovine serum albumin conjugated with fluorescein isothiocyanate was delivered via microinjection generally into the left atrial chamber. Subsequently, the images were recorded by videotape, and selected images in end diastole and end systole were digitized to allow quantitation of the left ventricular ejection fraction. In addition, separate injections were performed into the left ventricle to identify directly whether or not a shunt was present at the intraventricular level. Fig. 2 *A* and *B* displays representative fluorescent images of a normal RXRα +/+ embryo in diastole (Fig. 2*A*) and systole (Fig. 2*B*). The embryo is relatively translucent at this stage in development (E13.5), allowing direct visualization of cardiac contraction and relative orientation to the great vessels, including the ability to monitor blood flow. Note the reduction in size of the left ventricle during systole. Atrial chambers expand during ventricular systole (Fig. 2 *A* vs. *B*). This is primarily due to antegrade atrial filling, but underdevelopment of the AV cushions could also contribute if mitral regurgitation occurred. The heart rate can be monitored readily, with a closed chest serving as a reference for the open chest. Analysis also allowed scoring for AV synchrony and gross morphology of the heart, which in wild-type embryos are already relatively symmetrical elliptical chambers analogous to the adult.

Contractile Dysfunction in RXRα −/− Mice. Using this technology to monitor contractile function in RXRα −/− mice, matings were set up between mice that were heterozygous for the gene-targeted allele. Subsequently, litters (composed of wild-type, heterozygous, and homozygous mice) were examined at E13.5 or E14.5 to yield successful fluorescent studies in a total of 5 wild-type, 18 heterozygous, and 10 homozygous embryos.

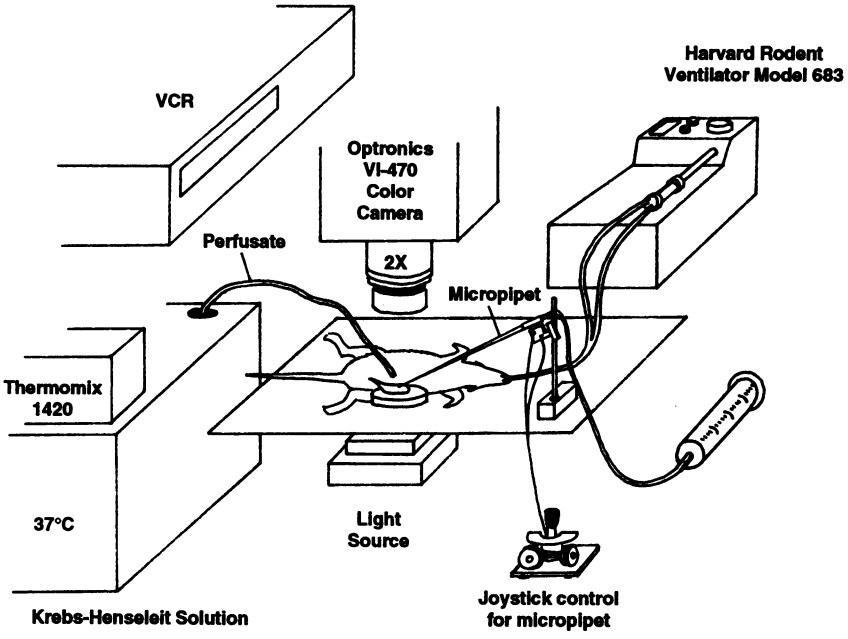

FIG. 1. Schematic diagram of the setup of the functional studies.

Normal wild-type (+/+) or heterozygote (+/−) hearts with small estimated left ventricular volumes considered due to an apex view of the heart leading to foreshortening artifact were eliminated. In some wild-type embryos, fluorescent albumin injections were unsuccessful and ejection fractions could not be calculated. Data for E13.5 were combined with E14.5 since there was no statistical difference between ejection fractions of the two different embryonic days of development. As shown in Fig. 3, the left ventricular area ejection fractions of the wild-type hearts at E13.5 and E14.5 averaged 50%. Also, the

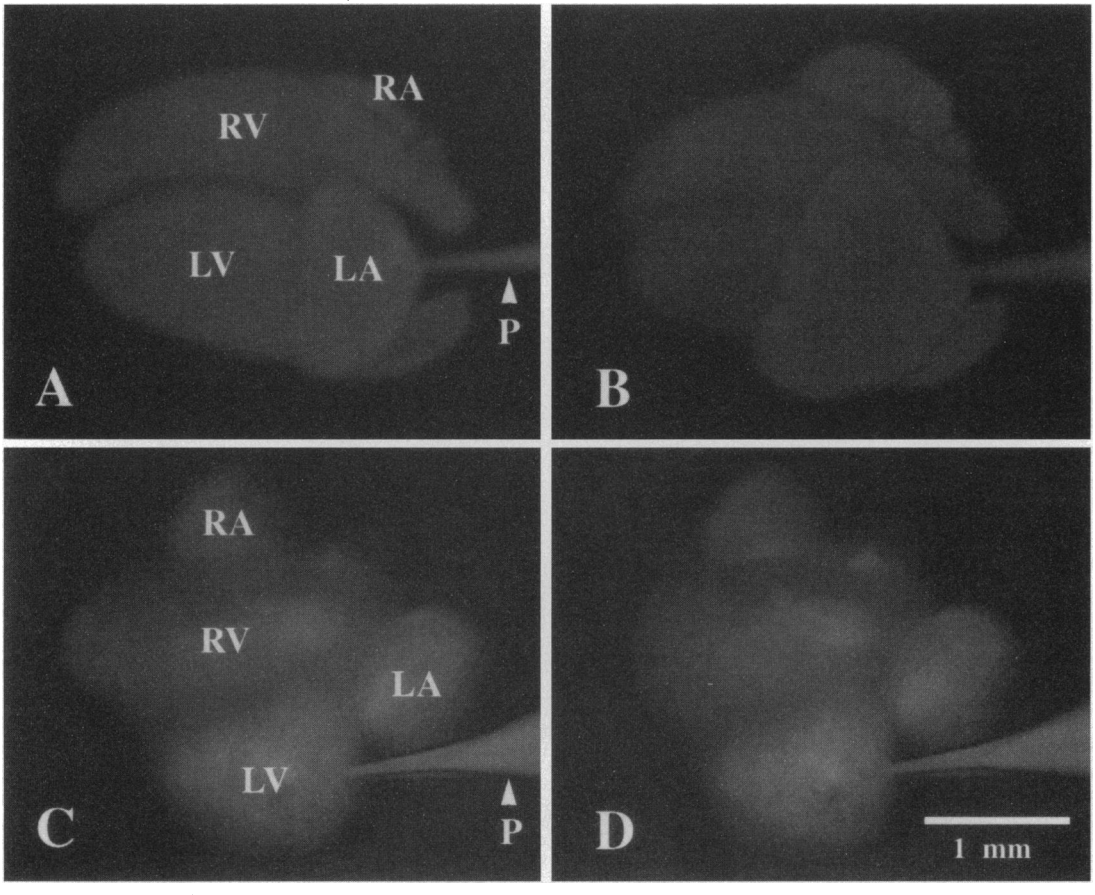

FIG. 2. Fluorescent video images. (*A* and *B*) Fluorescent images of normal heart. (*A*) Ventricular diastole. (*B*) Ventricular systole. (*C* and *D*) Fluorescent images of a RXRα −/− heart. (*C*) Ventricular diastole. (*D*) Ventricular systole. RV, right ventricle; LV, left ventricle; RA, right atrium; LA, left atrium; P, micropipette.

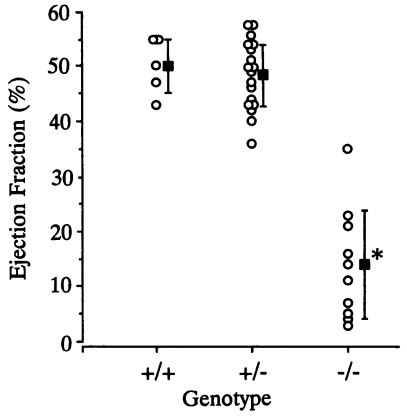

FIG. 3. Area ejection fractions of the left ventricle in E13.5 and E14.5 RXRα embryos. Ejection fractions were calculated as described. Data for E13.5 and E14.5 were combined, as there was no statistically significant difference between ejection fractions at the two different embryonic days of development. Each point represents a single embryonic heart. Solid squares represent means ± SEM. Genotypes are as follows: +/+, wild type; +/−, heterozygous; −/−, homozygous mutant. *, Average area ejection fraction for homozygous embryos was significantly different from both wild-type and heterozygous embryo area ejection fractions ($P < 0.01$).

left ventricular ejection fractions averaged 48% at E13.5 and E14.5 in heterozygous (+/−) mice. Thus, the fluorescent high-speed video microscopy with microinjection of fluorescein-tagged albumin appears to be a valid approach to quantitate ventricular chamber function in the living embryo with placental circulation intact.

Fig. 2 *C* and *D* displays representative fluorescent images of a homozygous mutant RXRα embryo in diastole (Fig. 2*C*) and systole (Fig. 2*D*). As shown, the size of the left ventricle of the mutant RXRα illustrates a very marked reduction of systolic ejection during systole. In addition, the RXRα −/− heart appeared much more transparent than the wild-type heart on color imaging (data not shown). Histological sections of hearts from embryos used for video imaging (data not shown) confirm this and are consistent with previously published work by Sucov *et al.* (10). As shown in Fig. 3, studies at E13.5 or E14.5 revealed the area ejection fractions of the left ventricles of the RXRα −/− embryos to average 14% (range, 3–35% for E13.5 and 4–23% for E14.5), representing a 72% decrease compared to +/+ and +/− embryos. In contrast, heterozygote embryos (RXR +/−) displayed relatively normal area ejection fractions within these litters.

The atrial structure and function as well as the overall position of the heart and great vessels appeared to be relatively normal between all groups (wild type, heterozygous, and homozygous), except in E14.5 embryos where the left atrium appeared small in −/− hearts (Fig. 2*A* vs. *C*). Whether or not reduced left atrial size was due to underdevelopment at that chamber or perhaps to low blood flow and inadequate time for secondary enlargement to occur prior to the death of the embryo is uncertain. Analysis of ventricular morphology by light-field microscopy of five RXRα −/− hearts revealed a globular rather than elliptical shape of both ventricles, reminiscent of a dilated form of congestive heart failure seen in the adult heart context. RXRα +/− hearts appeared to have normal chamber morphology.

Conduction Properties in RXRα −/− Embryos. Light-field analysis of embryonic heart function allowed evaluation of AV synchrony at these two different windows of murine embryonic development. At E13.5 and E14.5, the wild-type and heterozygous embryonic hearts all displayed normal AV synchrony. At E13.5, RXRα −/− embryos also displayed normal AV synchrony and had heart rates comparable to wild type. Heart rates averaged 120 (range, 60–176) beats per min in +/+ and +/− animals and 82 (range, 72–104) beats per min in −/− embryos. The comparable heart rate and the diminished ejection fraction at E13.5 suggests that the concomitant decrease in cardiac output in the RXRα −/− embryonic hearts is primarily related to the decreased cardiac ventricular contractile function, as opposed to a primary effect on slowing heart rate. However, by E14.5, the RXRα −/− embryos displayed a somewhat lower heart rate and an intermittent partial AV block (which was not quantified); there were two homozygous embryos that had complete heart block. Thus, at the later stage, the decreased rate of ventricular contraction may have contributed to some degree to the overall decrease in left ventricular function, but the profound depression of the ejection fraction was undoubtedly related to the thin left ventricular wall and impaired shortening of the myocardium in the RXRα −/− embryos. Since the development of the ventricular conduction system takes place during this stage of murine cardiogenesis (E11.0–E14.0) (15), the possibility exists that RXRα-dependent pathways might be required for normal maintenance of AV conduction. Whether the varying degrees of block reflect an indirect effect on conduction system network within the ventricular chamber, an intrinsic defect within the myocytes, or is the result of an anatomic defect at higher levels of the conduction system (i.e., the AV junction) remains to be determined.

Assessment of Ventricular Specification and Maturation in RXRα −/− Embryos via MLC-2 *in Situ* Analysis. Recent studies have used the atrial and ventricular chamber-specific MLC-2 genes as molecular markers for the process of chamber maturation and specification (13, 14). Within the embryonic and adult heart, the ventricular isoform MLC-2v is expressed exclusively in the ventricular chamber with negligible expression in the atrial compartment. This regional specification of MLC-2v expression occurs early during cardiogenesis, as positional specification of MLC-2v expression to the ventricular segment is found in the linear heart tube (E8.5) (13).

The expression of the atrial isoform MLC-2a appears to be uniform throughout the linear heart tube and then is selectively down-regulated in the ventricular chamber during the process of the expansion of the compact zone and the onset of trabeculation (14). In this manner, MLC-2a expression is a negative marker for the process of ventricular maturation, which occurs during E10.5–E13.5. To determine whether the muscle cells from RXRα −/− hearts would display defects in either ventricular specification or maturation, *in situ* hybridization analyses were performed with MLC-2a and MLC-2v RNA probes. *In situ* hybridization using antisense RNA probes revealed that specification of MLC-2v to the ventricular compartment of the heart in the RXRα −/− knockout embryos was appropriately maintained (Fig. 4 *A, B, E,* and *F*), a finding confirmed in a series of seven separate experiments in which the ventricular isoform of MLC-2 was appropriately restricted to the ventricular compartment (data not shown). However, in the adjacent sections from the same embryos, we found that there was aberrant, persistent expression of MLC-2a in the relatively thin-walled ventricular chambers (Fig. 4 *G* and *H*). In contrast, the wild-type littermate had already down-regulated the MLC-2a in the ventricular chamber and displayed background levels of expression (Fig. 4 *C* and *D*). These studies provide further evidence of a qualitative defect in the ventricular muscle cells found in the RXRα −/− mice, where there appears to be persistent expression of an atrial marker that is correlated with the relatively thin-walled atrial-like phenotype of the ventricular muscle cells, and establish MLC-2a as a convenient molecular marker of this atrial-like phenotype of the RXRα −/− embryos.

In summary, the present study provides direct evidence that the RXRα −/− embryos display embryonic heart failure that

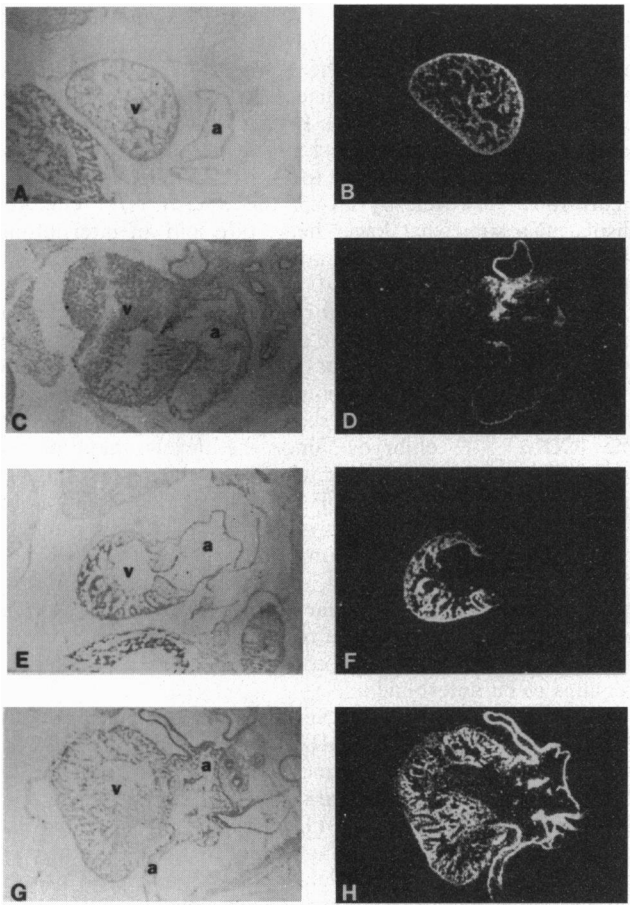

FIG. 4. *In situ* hybridization of E13.5 RXRα embryos. (*A*) Bright-field image of a wild-type RXRα embryo. (*B*) Dark-field image of *A* hybridized with the MLC-2v RNA probe. (*C*) Bright-field image of a wild-type RXRα embryo. (*D*) Dark-field image of *C* after hybridization with the MLC-2a RNA probe showing appropriate restriction of the MLC-2a message to the atrial compartment. (*E*) Bright-field image of a homozygous mutant RXRα embryo. (*F*) Dark-field image of *E* hybridized with the MLC-2v RNA probe showing appropriate restriction of MLC-2v expression to the ventricular chamber. (*G*) Bright-field image of a homozygous mutant RXRα embryo. (*H*) Dark-field image of *G* after hybridization with the MLC-2a RNA probe showing aberrant expression of MLC-2a in the ventricular chamber. v, Ventricle; a, atrium.

initially manifests itself as a decrease in ventricular contractile function. The dysfunction is progressive in the ventricular chamber, while atrial structure and function remain relatively intact. Evidence of atrial–ventricular conduction block suggests the possibility that a RXRα-dependent pathway may be required for normal development of the ventricular conduction system. *In situ* analysis with chamber-specific MLC-2 genes provides evidence of normal ventricular specification of MLC-2v in the RXRα −/− embryonic heart, while MLC-2a is persistently expressed in the ventricular chamber. Thus, the maturation of ventricular muscle cells appears to be arrested at E11.5–E12.5, placing the requirement for RXRα in this developmental time window. The availability of both molecular and physiological markers for the RXRα −/− defects should prove valuable in identifying the signaling pathways that lie downstream of RXRα and that mediate these ventricular chamber defects. In the event that down-regulation of MLC-2a is directly under the control of RXRα, analysis of the functional significance of the RA response elements, which lie in the MLC-2a promoter region (P. Doevendans, S.W.K., and K.R.C., unpublished observations), could be instructive as to whether this event is mediated by RXR homodimer or heterodimer pathways. In addition, the miniaturized physiological technology to monitor cardiac flow and function should be useful in characterizing the cardiac developmental phenotypes, which arise in other gene-targeted mouse model systems.

This work was supported by grants from the National Heart, Lung, and Blood Institute (HL36139 and HL45069 to K.R.C. and HL46345 to K.R.C. and J.R.), the American Heart Association (91022170 to K.R.C.), and the National Institutes of Health (NIH) (HL10881 and HL43026 to G.W.S.-S. and HD27183 to R.M.E.). J.R. is a recipient of an endowed chair awarded by the San Diego County Chapter of the American Heart Association. S.W.K. is a recipient of an Individual NIH National Research Service Award. R.M.E. is an Investigator of the Howard Hughes Medical Institute at the Salk Institute for Biological Studies. E.D. was a recipient of a Bugher Fellowship from the American Heart Association.

1. Wilson, J. G. & Warkany, J. (1949) *Am. J. Anat.* **85,** 113–155.
2. Kessel, M. & Gruss, P. (1991) *Cell* **67,** 89–104.
3. Webster, W. S., Johnston, M. C., Lammer, E. J. & Sulik, K. K. (1986) *J. Craniofacial Genet. Dev. Biol.* **6,** 211–222.
4. Lammer, E. J., Chen, D. T., Hoar, R. M., Agnish, N. D., Benke, P. J., Braun, J. T., Curry, C. J., Fernhoff, P. M., Grix, A. W., Jr., Lott, I. T., Richard, J. M. & Sun, S. C. (1985) *N. Engl. J. Med.* **313,** 837–841.
5. Brannan, C. I., Perkins, A. S., Vogel, K. S., Ratner, N., Nordlund, M. L., Reid, S. W., Buchberg, A. M., Jenkins, N. A., Parada, L. F. & Copeland, N. G. (1994) *Genes Dev.* **8,** 1019–1029.
6. Charron, J., Malynn, B. A., Fisher, P., Stewart, V., Jeannotte, L., Goff, S. P., Robertson, E. J. & Alt, F. W. (1992) *Genes Dev.* **6,** 2248–2257.
7. Chen, Z., Friedrich, G. A. & Soriano, P. (1994) *Genes Dev.* **8,** 2293–2301.
8. Kreidberg, J. A., Sariola, H., Loring, J. M., Maeda, M., Pelletier, J., Housman, D. & Jaenisch, R. (1993) *Cell* **74,** 679–691.
9. Mendelsohn, C., Lohnes, D., Decimo, D., Lufkin, T., LeMeur, M., Chambon, P. & Mark, M. (1994) *Development (Cambridge, U.K.)* **120,** 2749–2771.
10. Sucov, H. M., Dyson, E., Gumeringer, C. L., Price, J., Chien, K. R. & Evans, R. M. (1994) *Genes Dev.* **8,** 1007–1018.
11. Kastner, P., Grondona, J. M., Mark, M., Gansmuller, A., LeMur, M., Decimo, D., Vonesch, J.-L., Dolle, P. & Chambon, P. (1994) *Cell* **78,** 987–1003.
12. Lee, K. J., Ross, R. S., Rockman, H. A., Harris, A., O'Brien, T. X., van Bilsen, M., Shubeita, H., Kandolf, R., Brem, G., Price, J., Evans, S. M., Zhu, H., Franz, W. M. & Chien, K. R. (1992) *J. Biol. Chem.* **267,** 15875–15885.
13. O'Brien, T. X., Lee, K. J. & Chien, K. R. (1993) *Proc. Natl. Acad. Sci. USA* **90,** 5157–5161.
14. Kubalak, S. W., Miller-Hance, W. C., O'Brien, T. X., Dyson, E. & Chien, K. R. (1994) *J. Biol. Chem.* **269,** 16961–16970.
15. Viragh, S. & Challice, C. E. (1977) *Dev. Biol.* **56,** 397–411.